Two-stage neural-network based prognosis models using pathological image and transcriptomic data: An application in hepatocellular carcinoma patient survival prediction

Zhucheng Zhan[1], Noshad Hossenei[2,] Olivier Poirion[3], Maria Westerhoff [4], Eun-Young Choi[4], Travers Ching[5], Lana X. Garmire[2, $]

[1]*School of Science and Engineering, Chinese University of Hong Kong Shenzhen Campus, Shenzhen, P.R. China*
[2]*Department of Computational Medicine and Bioinformatics, University of Michigan, Ann Arbor, MI, USA*
[3]*Department of Cellular and Molecular Medicine, UC-San Diego, La Jolla, CA, USA*
[4]*Department of Pathology, University of Michigan, Ann Arbor, MI, USA*
[5]*Adaptive Biotechnologies, Seattle, Washington, USA*
$ corresponding author, email: lana.garmire@med.umich.edu

Keywords: prognosis, survival, prediction, neural network, modelling, Cox proportional hazards, pathology, image, gene expression, omics, RNA-Seq, data integration

Abstract: Pathological images are easily accessible data type with potential as prognostic biomarkers. Here we extend Cox-nnet, a neural network based prognosis method previously used for transcriptomics data, to predict patient survival using hepatocellular carcinoma (HCC) pathological images. Cox-nnet based imaging predictions are more robust and accurate than Cox proportional hazards model. Moreover, using a novel two-stage Cox-nnet complex model, we are able to combine histopathology image and transcriptomics RNA-Seq data to make impressively accurate prognosis predictions, with C-index close to 0.90 and log-ranked p-value of 4e-21 in the testing dataset. This work provides a new, biologically relevant and relatively interpretable solution to the challenge of integrating multi-modal and multiple types of data, particularly for survival prediction.

1 INTRODUCTION

Previously, we developed a neural network model called Cox-nnet to predict patient survival, using transcriptomics data [1]. Cox-nnet is an alternative to the conventional methods, such as Cox proportional hazards (Cox-PH) methods with LASSO or ridge penalization. We demonstrated that Cox-nnet is more optimized for survival prediction from high throughput gene expression data, with comparable or better performance than other conventional methods, including Cox-PH, Random Survival Forests [2] and CoxbBoost [3]. Moreover, Cox-nnet reveals much richer biological information, at both the pathway and gene levels, through analysing the survival related "surrogate features" represented in the hidden layer nodes in Cox-nnet.

One of the questions remaining unexplored, is whether other data types that previously have been shown prognostic values are also good input features to be exploited by Cox-nnet. One of such data types is pathological image data, eg. H&E staining data. These images are much more easily accessible and cheaper to obtain, compared to RNA-Seq transcriptomics data.

Therefore in this study, we extend Cox-nnet to take up pathological image features extracted from imaging processing tool *CellProfiler [4]*, and compare the predictive performance of Cox-nnet relative to Cox proportional hazards, the second best method in the original study. Moreover, we also propose a new kind of 2-stage complex Cox-nnet model as the proof-of-concept. The 2-stage Cox-nnet model combines the hidden node features from the 1st-stage of Cox-nnet models in parallel, where each Cox-nnet model is optimized to fit either image or RNA-Seq based data, and then use these combined features as the input nodes to train a 2nd-stage Cox-nnet model. We applied the models on TCGA hepatocellular carcinoma (HCC), which we had previously processed data and accumulated experience [5] [6] . In summary, our work here not only extends the previous Cox-nnet model to process pathological imaging data, but also creatively

addresses the multi-modal data integration challenges for patient survival prediction.

2 METHODS

2.1 Datasets

The histopathology images and their associated clinical information are downloaded from The Cancer Genome Atlas (TCGA). A total of 384 liver tumor images are collected. Among them 322 samples are clearly identified with tumor regions by pathology inspection. Among these samples, 290 have gene expression RNA-Seq data, and thus are selected for pathology-gene expression integrated prognosis prediction. The gene expression RNA-Seq dataset is also downloaded from TCGA, each feature was then normalized into RPKM using the function *ProcessRNASeqData* by TCGA-Assembler.

2.2 Tumor Image Processing

For each image, the tumor regions are labelled by pathologists at University of Michigan. The tumor regions are then extracted using Aperio software *ImageScope[7]*. To reduce computational complexities, each extracted tumor region is divided into non-overlapping 1000 by 1000 pixel tiles. The density of each tile is computed as the summation of red, green and blue values, and 10 tiles with the highest density are selected for further feature extraction similar to others [8]. To ensure that the quantitative features are measured under the same scale, the red, green and blue value are rescaled for each images. Image #128 with the standard background color (patient barcode: TCGA-DD-A73D) is selected as the reference image for the others to be compared with. The means of red, green and blue values of the reference image are computed and the rest of the images are normalized by the scaling factors of the its means of red, green, blue values relative to those of the reference image.

2.3 Feature Extraction from Image Set

CellProfiler is used for feature extraction [14]. Images are first preprocessed by '*UnmixColors*' module to H&E stains for further analysis. '*IdentifyPrimaryObject*' module is used to detect unrelated tissue folds and then removed by '*MaskImage*' module to increase the accuracy for detection of tumour cells. Nuclei of tumour cells are then identified by *'IdentifyPrimaryObject'* module again with parameters set by Otsu algorithm. The identified nuclei objects are utilised by '*IdentifySecondaryObject*' module to detect the cell body objects and cytoplasm objects which surround the nuclei. Related biological features are computed from the detected objects, by a series of feature extraction modules, including *'MeasureGranularity'*, *'MeasureObjectSizeShape'*, *'MeasureObjectIntensity'*, *'MeasureObjectIntensityDistribution'*, *'MeasureTexture'*, *'MeaureImageAreaOccupied'*, *'MeasureCorrelation'*, *'MeasureImageIntensity'* and *'MeasureObjectNeighbors*'. To aggregate the features from the primary and secondary objects, the related summary statistics (mean, median, standard deviation and quartiles) are then calculated to summarize data from object level to image level, yielding 2429 features in total. Each patient is represented by 10 images, and the median of each feature is selected to represent the patient's image biological feature.

2.4 Survival prediction models

Cox-nnet: The Cox-nnet model is implemented in the Python package named Cox-nnet [1]. Current implementation of Cox-nnet is a fully connected, two-layer neural network model, with a hidden layer and an output layer for cox regression. The drop-out method is used to avoid overfitting. We used hold-out method by randomly splitting the dataset to 80% training set and 20% testing set. We used grid search and 5-fold cross-validation to optimise the hyper-parameters for the deep learning model on the selected training set. The model is then trained under the optimised hyperparameter setting using the training set and further evaluated on the remaining testing set, the procedure is repeated 5 times to assess the average performance. More details about Cox-nnet is described earlier in Ching et al [1].

Cox proportional hazards Model: Since the number of features produced by *CellProfiler* exceed the sample size, an elastic net Cox proportional hazard model is built to select features and compute the prognosis index (PI) [9]. Function *cv.glmnet* in the *Glmnet* R package is used to performs cross-validation to select the tuning parameter *lambda*. The parameter *alpha* that controls the trade-off between quadratic penalty and linear penalty is selected using grid search. Same hold-out setting is employed by training the model using 80% randomly selected data and evaluated on the remaining 20% testing set. The procedure is repeated 5 times to calculate the mean accuracy of the model.

2.5 Model evaluation

Similar to the previous studies [1][5][6], we also use concordant index (C-index) and log-ranked p-value as the metrics to evaluate model accuracy. C-index signifies the fraction of all pairs of individuals whose predicted survival times are correctly ordered and is based on Harrell C statistics. Conventionally, a C-index around 0.70 indicates a good model, whereas a score around 0.50 means randomness. As both Cox-nnet and Cox-PH model quantify the patient's prognosis by log hazard ratios, we use the predicted median hazard ratios to stratify patients into two risk groups (high vs. low survival risk groups). We also compute the log-rank p-value to test if two Kaplan-Meier survival curves produced by the dichotomised patients are significantly different.

2.6 Feature evaluation

The input feature importance score is calculated by drop-out. The values of a variable are set to its mean and the log likelihood of the model is recalculated. The difference between the original log likelihood and the new log likelihood is considered as feature importance [13]. We select 100 features with the highest feature scores from Cox-nnet for association analysis between pathology image and gene expression features. We regress each selected image feature (y) over all the gene expression features (x) using LASSO penalization, and then use the R-square statistic as the correlation metric.

2.7 Data integration

We construct 1st-stage Cox-nnet models using the image data and gene expression data of HCC, respectively. For each model, grid search is used on the training set to optimize the hyper-parameters under 5-fold cross-validation. Then we extract and combine the nodes of the hidden layer from each Cox-nnet model as the new input features for the 2nd-stage model. This new Cox-nnet model is constructed and evaluated with the same parameter-optimization strategies.

3 RESULTS

3.1 Overview of Cox-nnet model on pathological image data

In this study, we tested if pathological images can be used to predict cancer patient survival. As described in the Methods, pathological images of 322 TCGA HCC patients are individually annotated with tumor contents by pathologists, before being subject a series of processing steps. The tumor regions of these images then undergo segmentation, and the top 10 tiles (as described in section 2.2) out of 1000 by 1000 tiles are used to represent each patient. These tiles are next normalized for RGB coloring against a common reference sample, and 2429 image features of different categories are extracted by *CellProfiler*. Summary statistics (mean, median, standard deviation and quartiles) are calculated for each image features, and the median values of them over 10 tiles are used as the input imaging features for survival prediction.

We applied these imaging features on Cox-nnet, a neuron-network based prognosis prediction method previously developed by our group. The architecture of Cox-nnet is shown in **Figure 1.** Briefly, Cox-nnet is composed of the input layer, one fully connected hidden layer and an output "proportional hazards" layer. We use 5-fold cross-validation (CV) to find the optimal regularization parameters. Based on the results on RNA-Seq transcriptomics previously, we use dropout as the regularization method. Additionally, to evaluate the results on pathology image data, we compare Cox-nnet with Cox-PH model, the previously 2nd-best prognosis model on RNA-Seq data.

Figure 1: the architectures of Cox-nnet model: The sketch of Cox-nnet model for prognosis prediction, based on a single data type.

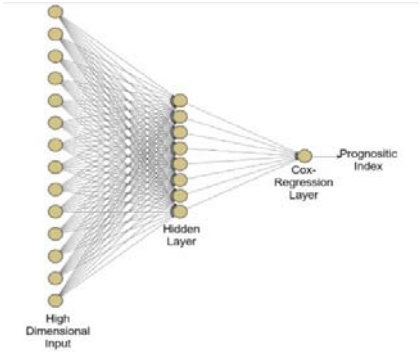

3.2 Comparison of prognosis prediction between Cox-nnet and Cox-PH over pathology imaging data

We use two accuracy metrics to evaluate the performance of models in comparison: C-index and log-rank P-values. C-index measures the fraction of all pairs of individuals whose predicted survival times are correctly ordered by the model. The higher C-index, the more accurate the prognosis model is. On the other hand, log-rank p-value tests if the two Kaplan-Meier survival curves based on the survival risk-stratification are significantly different (log-rank p-value <0.05). In this study, we stratify the patients by the median score of predicted prognosis index (PI) from the model. As shown in **Figure 2,** the C-index values from the Cox-PH model are much more variable (less stable), compared to those from Cox-nnet. Moreover, the median C-index score from Cox-nnet is higher (around 0.75) than Cox-PH (less than 0.70).

Figure 2: Comparison of prognosis prediction with different models and data types

Figure 3: Comparison of Kaplan-Meier survival curves resulting from Cox-PH and Cox-nnet models, based on pathological images.

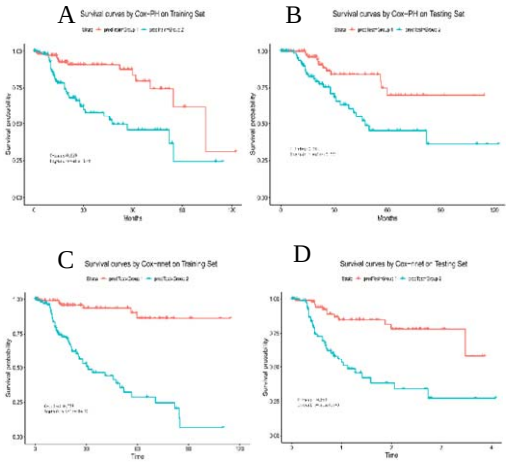

Additionally, the discrimination power of Cox-nnet on patient Kaplan-Meier survival difference (**Figure 3 C and D**) is much better than Cox-PH model (**Figure 3 A and B**), using median PI based survival risk stratification. In the training dataset, Cox-nnet achieves a log-rank P-value of 1e-13, compared to 3e-5 for Cox-PH; in the testing dataset, Cox-nnet achieves a log-rank P-value of 1e-6, whereas Cox-PH gives a result of 0.01.

We next investigated the top 100 image features according to Cox-nnet ranking (**Figure 4**). Interestingly, the most frequent features are those involved in textures of the image, accounting for 43% of raw input features. Intensity and Area/Shape parameters make up the 2nd and 3rd highest categories, with 21% and 15% features. Density, on the other hand, is less important (6%). It is also worthy to note that among 49 selected features from the conventional Cox-PH model, 63% (31) are also found in the top 100 features found by Cox-nnet.

Figure 4: Categories of the top 100 most important image features in Cox-nnet.

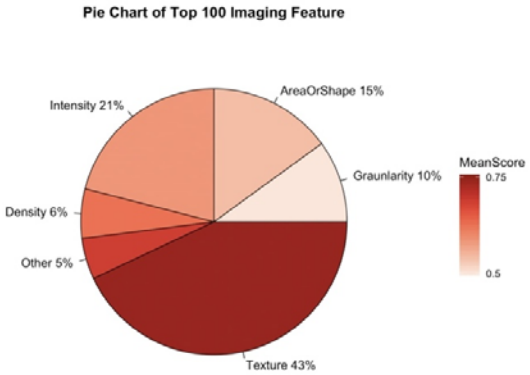

3.3 Prognosis prediction by combining histopathology imaging and gene expression RNA-Seq data

Multi-modal and multi-type data integration is challenging, particularly so for survival prediction. We next ask if we can utilize Cox-nnet workframe for such purpose, exemplified by pathology imaging and gene expression RNA-Seq based survival prediction.

Towards this, we propose a two-stage Cox-nnet complex model, inspired by other two-stage models

in genomics fields [10] [11] [12]. The two-stage Cox-nnet model is depicted in **Figure 5** below. For the first stage, we construct two Cox-nnet models in parallel, using the image data and gene expression data of HCC, respectively. For each model, we optimize the hyper-parameters using grid search under 5-fold cross-validation. Then we extract and combine the nodes of the hidden layer from each Cox-nnet model as the new input features for the second-stage Cox-nnet model. We construct and evaluate the second-stage Cox-nnet model with the same parameter-optimisation strategy as in the first-stage.

Figure 5: the architectures of 2-stage Cox-nnet complex model for prognosis prediction, which integrates multiple data types (eg. pathology image and gene expression).

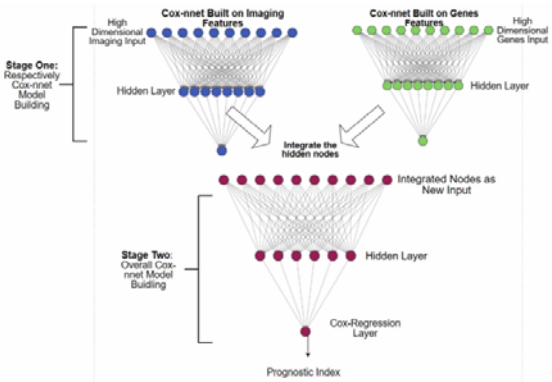

As shown in **Figure 6,** the resulting two-stage Cox-nnet model yields impressive performance, judged by the C-index values on both training set and testing set, both of which are close to 0.90. In fact, from our experience over the years, none of the prognosis models based on one omic data type had yielded a predictive C-index score nearly as high. This outstanding performance of the two-stage Cox-nnet model is also confirmed by the log-rank P-values in the Kaplan-Meier survival curves (**Figure 6**). In the training dataset, Cox-nnet achieves a log-rank P-value of 6e-17; in the testing dataset, Cox-nnet has an even higher log-rank P-value of 4e-21. The fact that the testing dataset obtains a better log-rank p-value than the training dataset, indicates that the over-fitting is less of a concern. Note: the C-index values in **Figure 6** are different from those in **Figure 2**, since the objective in these plots is to differentiate the stratified risk groups *post* the cox-nnet model, rather than fitting the survival data directly.

Figure 6: Kaplan-Meier survival curves resulting from the 2-stage Cox-nnet model, combining pathological images and gene expression RNA-Seq data from same HCC patients. A. training set. B. testing set.

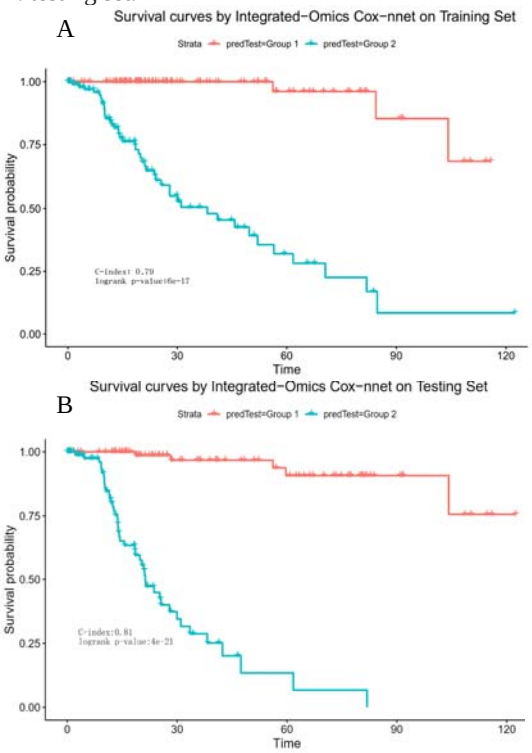

We also investigate the correlations between the top imaging features with those RNA-Seq gene expression features. For this we regress each selected image feature (y) over all the gene expression features (x) using LASSO penalization. Interestingly, among the top 20 imaging features, none but one feature (StDev_Nuclei_AreaShape_MajorAxisLength) has a decent correlation value (R-square=0.30) with gene expression features. This result shows that imaging features extracted using *CellProfiler* have mostly orthogonal (or non-overlapping) predictive information to the RNA-Seq gene expression features. This also supports the observed significant increase in C-index (**Figure 2**) and log-ranked p-values (**Figure 6**), after adding RNA-Seq features to imaging features.

4 CONCLUSIONS

Driven by the objective to build a uniform workframe to integrate multi-modal and multi-type data to predict patient survival, we extend Cox-nnet model, a neural-network based survival prediction method, on pathology imaging data and beyond. Using TCGA HCC pathology images as the example, we demonstrate that Cox-nnet is more robust and accurate at predicting testing dataset, relative to Cox-PH, the standard method for survival prediction (which was also the second-best method in the original RNA-Seq transcriptomic study [1]). Moreover, we propose a new two-stage complex Cox-nnet model to integrate imaging and RNA-Seq transcriptomic data, and show case its outstanding predictive accuracy on testing dataset (C-index almost as high as 0.90). The two-stage Cox-nnet model combines the transformed, hidden node features from the first-stage of Cox-nnet models for imaging or RNA-Seq based data respectively and use these combined features as the inputs to train a second-stage Cox-nnet model.

Rather than using convolutional neural network (CNN) models that are more complex, we utilized a less complex but perhaps more biologically relevant approach, where we extract imaging features using the tool *CellProfiler*. These features are then fed in a relatively simple, two-layer neural network model, and still achieve credible predictive performance. Such success argues that in biological domain, it is possible to use relatively simple neural network models with have prior biological relevance (such as in the input features). In summary, our work here not only extends the previous Cox-nnet model to process pathological imaging data, but also creatively addresses the multi-modal data integration challenges for patient survival prediction.

ACKNOWLEDGEMENTS

LXG would like to thank the support by grants K01ES025434 awarded by NIEHS through funds provided by the trans-NIH Big Data to Knowledge (BD2K) initiative (www.bd2k.nih.gov), R01 LM012373 and LM012907 awarded by NLM, R01 HD084633 awarded by NICHD to L.X. Garmire.

REFERENCES

[1] T. Ching, X. Zhu, and L. X. Garmire, “Cox-nnet: An artificial neural network method for prognosis prediction of high-throughput omics data,” PLoS Comput. Biol., vol. 14, no. 4, p. e1006076, Apr. 2018.

[2] H. Ishwaran and M. Lu, “Random Survival Forests,” Wiley StatsRef: Statistics Reference Online. pp. 1–13, 2019.

[3] R. D. Bin and R. De Bin, “Boosting in Cox regression: a comparison between the likelihood-based and the model-based approaches with focus on the R-packages CoxBoost and mboost,” Computational Statistics, vol. 31, no. 2. pp. 513–531, 2016.

[4] C. McQuin, A. Goodman, V. Chernyshev, L. Kamentsky, B. A. Cimini, K. W. Karhohs, M. Doan, L. Ding, S. M. Rafelski, D. Thirstrup, W. Wiegraebe, S. Singh, T. Becker, J. C. Caicedo, and A. E. Carpenter, “CellProfiler 3.0: Next-generation image processing for biology,” PLoS Biol., vol. 16, no. 7, p. e2005970, Jul. 2018.

[5] K. Chaudhary, O. B. Poirion, L. Lu, and L. X. Garmire, “Deep Learning-Based Multi-Omics Integration Robustly Predicts Survival in Liver Cancer,” Clin. Cancer Res., vol. 24, no. 6, pp. 1248–1259, Mar. 2018.

[6] K. Chaudhary, O. B. Poirion, L. Lu, S. Huang, T. Ching, and L. X. Garmire, “Multi-modal meta-analysis of 1494 hepatocellular carcinoma samples reveals vast impacts of consensus driver genes on phenotypes.” .

[7] C. Marinaccio and D. Ribatti, “A simple method of image analysis to estimate CAM vascularization by APERIO ImageScope software,” Int. J. Dev. Biol., vol. 59, no. 4–6, pp. 217–219, 2015.

[8] K.-H. Yu, C. Zhang, G. J. Berry, R. B. Altman, C. Ré, D. L. Rubin, and M. Snyder, “Predicting non-small cell lung cancer prognosis by fully automated microscopic pathology image features,” Nat. Commun., vol. 7, p. 12474, Aug. 2016.

[9] S. Huang, C. Yee, T. Ching, H. Yu, and L. X. Garmire, “A novel model to combine clinical and pathway-based transcriptomic information for the prognosis prediction of breast cancer,” PLoS Comput. Biol., vol. 10, no. 9, p. e1003851, Sep. 2014.

[10] T. Schulz-Streeck, J. O. Ogutu, and H.-P. Piepho, “Comparisons of single-stage and two-stage approaches to genomic selection,” Theor. Appl. Genet., vol. 126, no. 1, pp. 69–82, Jan. 2013.

[11] R. Wei, I. De Vivo, S. Huang, X. Zhu, H. Risch, J. H. Moore, H. Yu, and L. X. Garmire, “Meta-dimensional data integration identifies critical pathways for susceptibility, tumorigenesis and progression of endometrial cancer,” Oncotarget, vol. 7, no. 34, pp. 55249–55263, Aug. 2016.

[12] Pinu FR, Beale DJ, Paten AM, et al, “Systems Biology and Multi-Omics Integration: Viewpoints from the Metabolomics Research Community,”. Metabolites. 2019;9(4):76. Published 2019 Apr 18.

[13] Bengio Y, Boulanger-Lewandowski N, Pascanu R, editors. “Advances in optimizing recurrent networks,”

Acoustics, Speech and Signal Processing (ICASSP), 2013 IEEE International Conference on; 2013: IEEE.
[14] Kamentsky, L. et al. Improved structure, function and compatibility for CellProfiler: modular high-throughput image analysis software. Bioinformatics 27, 1179–1180 (2011).